Behavioral Analysis of Co-operative/Competitive Antibody Dynamics

Madhumala Ghosh, Amit Konar, L. C. Jain, and Uday K. Chakraborty

Abstract—**The paper presents an analysis of chaos, limit cycles and stability in the antigen-antibody interactive dynamics. Both co-operation and competition of antibodies are considered in the dynamics. The classical approach of Lyapunov has been employed here for the stability analysis of the dynamics. Computer simulations have been undertaken to support the results of the analysis. Both temporal behaviors of the antibodies and their phase portraits have been given to study their chaotic, limit cyclic and stable behavior. Results of stability analysis of the dynamics have been applied in a garbage cleaning problem by a mobile robot.**

I. INTRODUCTION

PIONEERED by Langton, artificial life [9] embraces human–made systems that posses some of the fundamental properties of natural life [10]. While studying artificial life, we are specifically interested in artificial systems that serve as models of living systems for the investigation of open questions in biology. Artificial immune systems (AIS) are biologically inspired models for immunization of engineering systems. The pioneering task of AIS is to detect and eliminate non-self materials, called "antigens" such as virus cells or cancer cells. The artificial immune system also plays a great role in maintaining its own system against a "dynamically changing environment" [19]. The immune system thus aims at providing a new methodology suitable for dynamics problems dealing with unknown/hostile environment.

In recent years, much attention has been focused on behavior-based AI for its proven robustness and flexibility in a dynamically changing environment. Artificial immune systems are one such behavior-based reactive system that aim at developing a decentralized consensus making mechanism, following the behavioral characteristics of biological immune systems.

The basic components of the biological immune system are macrophages, antibodies and lymphocytes, the last one being classified into two types: B-lymphocytes [5] and T-lymphocytes [5], which are the cells stemming from the bone marrow. The human blood circulatory system contains roughly 10^7 distinct types of B-lymphocytes, each of which has a distinct molecular structure and produces Y-shaped [5] antibodies from its surface. Antibodies can recognize foreign substances, called antigens that invade living creature. Virus, cancer cells etc. are typical examples of antigens. To cope with continuously changing environment, living systems possess enormous repertoire of antibodies in advance. T-lymphocytes, on the other hand, are the cells maturing in thymus, and they are used to kill infected cells and regulate the generation of antibodies from B-lymphocytes as outside circuits of B-lymphocyte networks [19]. It is interesting to note that an antibody recognizes an antigen by part of its structure called epitope [5]. The portion of the antibody that has the recognizing capability of an antigen is called paratope [5]. Usually, epitope is the key portion of the antigen, and paratope is the keyhole portion of the antibody. Recent studies in immunology reveal that each type of antibody has its specific antigen-determinant, called idiotope [5].

The simple model of antibody dynamics presumes immediate interaction between antibody i and antibody j. However, the growth of concentration of antibody i starts after a small depletion of antibody j. Further, antibody i has a maximum concentration label K determined by our blood vessels and biomass. With these two points in mind, we consider a new model of antibody dynamics that demonstrates co-operation between antibody i and j and competition of antibody i with antibody k to interact with antigen m. We ignore the decay term of the basic antibody dynamics [7] as the maximum carrying capacity K of an antibody by blood vessels and biomass has already been taken into account. It is indeed important to note that such dynamics results in chaotic, limit cyclic or stable behavior. A chaotic response is indicated by a random non-periodic fluctuation of antibody concentration over time. A limit cyclic behavior is identified from its periodic temporal oscillation, whereas stability ensures convergence of the antibody concentration towards a fixed value. When all the antibodies attain stability, the dynamics is said to have reached a stable/equilibrium point. In this paper, we determine the stability condition of the antibody dynamics using Lyapunov energy functions, and verify chaotic state of the dynamics by using the Lyapunov exponent. Chaos and limit cycles are undesirable in the temporal behavior of antibody dynamics. In this paper, we utilize the stable behavior of antibody dynamics for a garbage cleaning application by mobile robots. The paper has been

Madhumala Ghosh is with the Department of Electronics and Tele-Communication Engineering, Jadavpur University, Kolkata 700 032, India (phone: 91-33-32527447; e-mail: madhumala_ghosh@rediffmail.com).

Amit Konar is with the Department of Electronics and Tele-Communication Engineering, Jadavpur University, Kolkata 700032, India (e-mail: konaramit@yahoo.co.in).

L. C. Jain is with Knowledge-Based Intelligent Engineering Systems Centre, University of South Australia, Adelaide, SA-5095, Australia (e-mail: lakhmi.jain@unisa.edu.au).

Uday K. Chakraborty is with Department of Mathematics & Computer Science, University of Missouri, St. Louis, MO 63121, USA (phone: +1 314 516 6339; e-mail: uday@cs.umsl.edu).

978-1-4244-1823-7/08/$25.00©2008 IEEE

divided into six sections. In section II, we propose a new model of antibody dynamics and analyze the temporal behavior of the dynamics by varying the parameters. In section III, we determine the conditions for stability of the dynamics by using a suitable Lyapunov energy function. The parameter settings for chaos of the dynamics are verified in section IV with the help of a Lyapunov exponent. An application of the stable behavior of the model is studied in section V for the well-known garbage collection problem [19] by a mobile robot. Conclusions are listed in section VI.

II. THE PROPOSED MODEL FOR ANTIBODY–ANTIGEN INTERACTIVE DYNAMICS AND ITS BEHAVIORAL ANALYSIS

Existing models of AIS are pivoted around the growth dynamics of an antibody as a non–linear function of co-operative and competitive antibodies' strength, induced by the specific antibody under consideration [24]. The interaction between an antigen and a given antibody, and the self-decay rate of the antibody are taken into account in the antibody dynamics. A squashing function is used to offer an inhibiting action to the growth of an antibody. In this paper, we however consider an extension of the basic model referred to above. The extension is considered in the co-operative and competitive terms of the individual antibodies, over the growth dynamics of an antibody i.

A. The Model

Let

X_i be the concentration of antibody i,

Y_m be the concentration of antigen j,

b_{ji} be the co-operative strength of antibody j on antibody i,

c_{ki} be the competitive strength of antibody 'k' on antibody i,

z_{im} be the strength of affinity of antibody i on antigen m,

a_{ii} be the growth rate of antibody i,

and K denote the carrying capacity of the antibody 'i' by the blood vessels or biomass.

We presume that the co-operation (competition) of an antibody j (antibody k) starts after a certain depletion of the antibody j (antibody k). This depletion has been represented by an exponentially rising factor, called influence, defined over the self-growth of the antibody. The influence of a co-operative antibody j or competitive antibody k to antibody i controls the growth rate of antibody i. The natural decay rate of antibody i is ignored in this paper for simplicity. The interaction between antibody i and antigen m is considered by an additional term in the dynamics of the i th antibody.

Therefore, for at least one co-operative antibody of j type, the growth rate in concentration of antibody i can be written as:

$$\frac{dX_i}{dt} = \sum_{\exists j} b_{ji} X_i (1 - \exp(-\beta_{ji} X_j)) \tag{1}$$

where β_{ji} denotes the depletion rate of antibody j that influences the growth in antibody i.

In the same manner, competition by at least one antibody of k type, the growth dynamics of antibody i is given by

$$\frac{dX_i}{dt} = \sum_{\exists k} c_{ki} X_i (1 - \exp(-\lambda_{ik} X_k)) \tag{2}$$

where λ_{ik} denotes the depletion rate of antibody k that influences the growth rate in antibody i.

When growth in antibody i depends on the concentration of at least one antigen m, the dynamics of antibody i is given by

$$\frac{dX_i}{dt} = \sum_{\exists m} z_{im} X_i Y_m \ . \tag{3}$$

Since the carrying capacity of antibody i is K, the growth rate in antibody i will be positive when $X_i < K$, negative when $X_i > K$, and zero when $X_i = K$. Mathematically, we write this as

$$\frac{dX_i}{dt} = a_{ii} X_i (1 - \frac{X_i}{K}) \ . \tag{4}$$

When all the above four phenomena, such as co-operation by antibody of j type and competition by antibody of k type occurs in presence of antigen of m type, and natural growth rate of antibody is considered, the dynamics of antibody i is given by

$$\begin{aligned}\frac{dX_i}{dt} = {} & a_{ii} X_i (1 - \frac{X_i}{K}) + \sum_{\exists j} b_{ji} X_i (1 - \exp(-\beta_{ji} X_j)) \\ & - \sum_{\exists k} c_{ki} X_i (1 - \exp(-\lambda_{ik} X_k)) + \sum_{\exists m} z_{im} X_i Y_m \ .\end{aligned} \tag{5}$$

In this paper, we consider the above model for antigen-antibody interactive dynamics.

B. Behavioral analysis of antibody dynamics

In this section, we study the temporal behavior of antibody dynamics through numerical solution of the non-linear differential equation. For convenience, we consider four antibodies and four antigens. The complete dynamics is given in equations (6)-(9).

$$\begin{aligned}\frac{dX_1}{dt} = {} & a_{11} X_1 (1 - \frac{X_1}{K}) + b_{31} X_1 (1 - \exp(-\beta_{31} X_3)) \\ & - c_{12} X_1 (1 - \exp(-\lambda_{21} X_2)) + z_{11} X_1 Y_1\end{aligned} \tag{6}$$

$$\begin{aligned}\frac{dX_2}{dt} = {} & a_{22} X_2 (1 - \frac{X_2}{K}) + b_{12} X_2 (1 - \exp(-\beta_{12} X_1)) \\ & + b_{42} X_2 (1 - \exp(-\beta_{42} X_4)) - b_{32} X_2 (1 - \exp(-\beta_{32} X_3)) \\ & - c_{23} X_2 (1 - \exp(-\lambda_{32} X_3)) + z_{22} X_2 Y_2\end{aligned} \tag{7}$$

$$\begin{aligned}\frac{dX_3}{dt} = {} & a_{33} X_3 (1 - \frac{X_3}{K}) + b_{23} X_3 (1 - \exp(-\beta_{23} X_2)) \\ & - c_{32} X_3 (1 - \exp(-\lambda_{23} X_2)) - c_{31} X_3 (1 - \exp(-\lambda_{13} X_1)) \\ & - c_{34} X_3 (1 - \exp(-\lambda_{43} X_4)) + z_{33} X_3 Y_3\end{aligned} \tag{8}$$

$$\begin{aligned}\frac{dX_4}{dt} = {} & a_{44} X_4 (1 - \frac{X_4}{K}) + b_{34} X_4 (1 - \exp(-\beta_{34} X_3)) \\ & - c_{42} X_4 (1 - \exp(-\lambda_{24} X_2)) + z_{44} X_4 Y_4\end{aligned} \tag{9}$$

We now study the effect of variation of the parameters a_{ii}, b_{ji}, c_{ki}, and z_{im} for $1 \le i \le 4$, $1 \le j \le 4$, $1 \le k \le 4$, $1 \le m \le 4$.

III. EFFECT OF VARIATION IN PARAMETERS OF THE ANTIGEN-ANTIBODY DYNAMICS

Variation in a_{ii}: a_{ii} plays an important role in the stabilization of the said antigen-antibody dynamics. It has been noted (Fig. 1) that keeping the other parameters of the dynamics constant, as indicated in Table I, a large variation in a_{11} forces the system to have a limit cyclic (when a_{11}=0.15) or chaotic behavior (when a_{11}>0.33). When a_{22} or a_{33} increases, stabilization of the overall system is hampered. Further, on increase in a_{44} (when a_{44}>0.21) the stability of the overall system dynamics is increased.

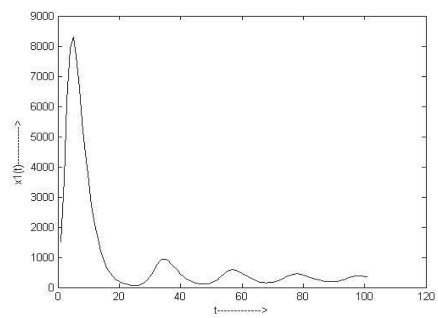

(a) Stable behavior of $X_1(t)$ for a_{11}=0.03;

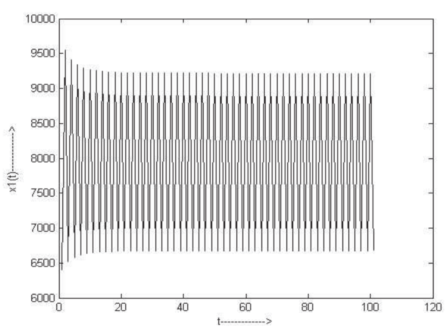

(b) Limit Stable behavior of $X_1(t)$ for a_{11}=0.15;

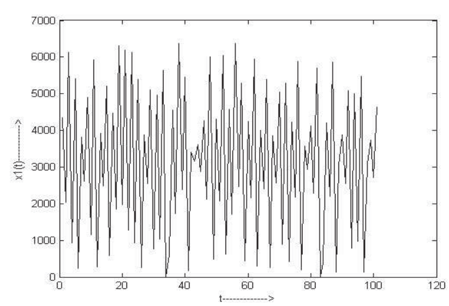

(c) Chaotic behavior of $X_1(t)$ for a_{11}=0.33

Fig. 1: Temporal dynamic behavior of X_1 vs. time to indicate (a) stable, (b) limit cyclic and (c) chaotic behavior for different values of a_{11}. The other parameters of the dynamics are included in TABLE I and II.

Variation in b_{ji}: Computer simulations reveal that a decrease in b_{31} below 0.5 keeping all other parameters fixed, as indicated in TABLE I and II, retains the oscillatory nature of the antigen-antibody dynamics (Fig. 2). When b_{31} is increased up to 0.9, the oscillation in all the antibody concentration X_1, X_2, X_3, and X_4 are sustained. When b_{31} is increased further to 1.0, the oscillation dies out and all the states of the antigen-antibody dynamics attain equilibrium. The phenomenon for sustaining oscillation at small values of b_{ji} and maintaining equilibrium at values higher than b_{ji} are explained as follows; When b_{31} is smaller than 0.9, the positive feedback provided by the antigen-antibody dynamics is inadequate to maintain large amplitude in X_1 because of a large negative feedback from other states. Naturally the dynamics of X_3 and X_4, which are strongly influenced by X_2, have similar behavior like X_2.

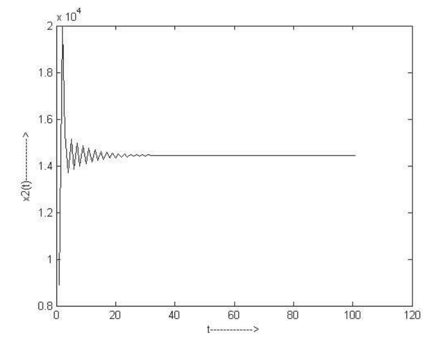

(a) Stable behavior of $X_2(t)$ for b_{12}=0. 215

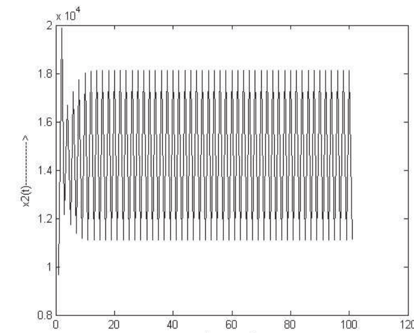

(b) Limit cyclic behavior of $X_2(t)$ for b_{12}=0. 3

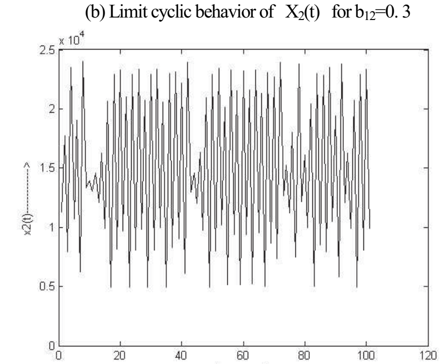

(c) Chaotic behavior of $X_2(t)$ for b_{12}=0.5;

Fig. 2: Temporal dynamic behavior of X_2 vs. time to indicate (a) stability, (b) limit cyclic and (c) chaotic behavior for different values of b_{12}. The other parameters of the dynamics are included in TABLE I and II.

Variation in c_{ki}: Decreasing the value of c_{12} from 0.55 reduces the oscillatory nature of the dynamics. When c_{12}

attains 0.35, there exists an overshoot in the under-damped case, but oscillations die out. Apparently this seems to be counter-intuitive, as a decrease in c_{12} causes a relative increase in the growth rate of X_1, causing over-arousal in X_1. In fact, the same thing happens in the transient phase, but in the steady-state phase, the increased growth rate of X_1 suppresses the arousal of X_2, X_3, and X_4 states. Consequently, decreasing c_{12} stabilizes the behavior of all the antigen-antibody states. It has been noted that when c_{12} is decreased to 0.01, all the states return to the equilibrium state. An increase in c_{12} pushes the dynamics towards limit cyclic behavior and further increment of this parameter results in stabilization of the whole dynamics (Fig. 3).

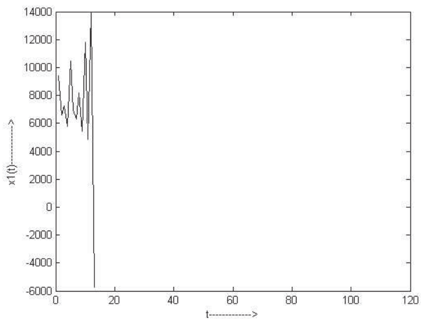

(a) Stable behavior of $X_1(t)$ for c_{12}=0.005

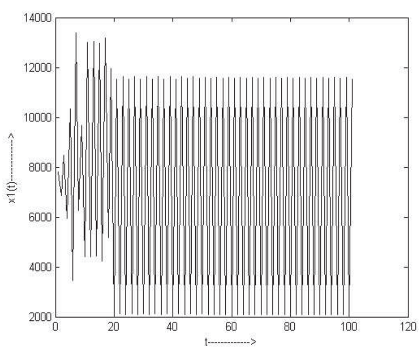

(b) Limit Stable behavior of $X_1(t)$ for c_{12}=0.35

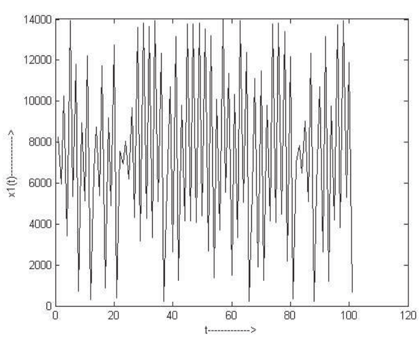

(c) Chaotic behavior of $X_1(t)$ for c_{12}=0.27

Fig. 3: Temporal dynamic behavior of X_1 vs. time to indicate (a) stability, (b) limit cyclic and (c) chaotic variations for different values of c_{12}. The other parameters of the dynamics are included in TABLES I and II.

Variation in z_{im}: z_{im} plays an important role in the stabilization of the said antigen-antibody dynamics. It has been noted that keeping the other parameters of the dynamics constant (as indicated in TABLE I and II), a large variation in z_{11} forces the system to a limit cycles or chaos. When the value of z_{11} is 0.001, the system is totally stable in behavior, but when it reaches 0.004, and above, the system behavior exhibits limit cyclic behavior. When z_{11}= 0.005, and above, the dynamics becomes chaotic. When z_{22} or z_{33} increases, stabilization of the overall system is hampered. Further on increase in z_{44} the stability of the overall system dynamics is increased.

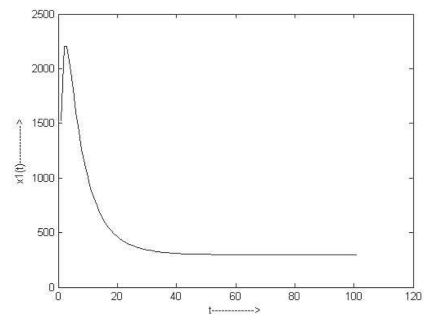

(a) Stable behavior of $X_1(t)$ for z_{11}=0.001

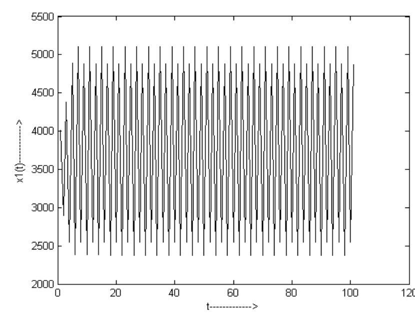

(b) Limit Stable behavior of $X_1(t)$ for z_{11}=0.0045

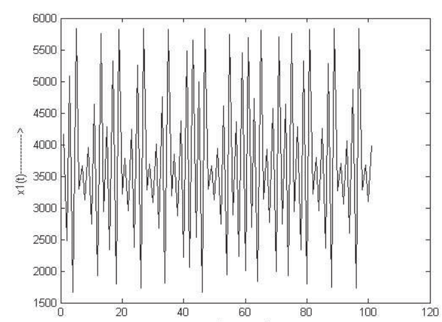

(c) Chaotic behavior of $X_1(t)$ for z_{11}=0.0048

Fig. 4: Temporal dynamic behavior of X_1 vs. time to indicate (a) stability, (b) limit cyclic and (c) chaos for different values of z_{11}.
The other parameters of the dynamics are included in TABLES I and II.

Variation in β_{ji}: In antigen-antibody dynamics β_{ji} has a major role in controlling the stability of the whole dynamics.

When the value of β_{ji} increases, the system results in limit cyclic behavior, and on further increase of β_{ji}, the dynamics becomes chaotic (Fig. 5).

Variation in λ_{ik}: The behavior of λ_{ik} is totally opposite in comparison to other parameters. When we increase the value of λ_{ik}, the system becomes stable but on decreasing its value the system behavior will be chaotic (Fig. 6).

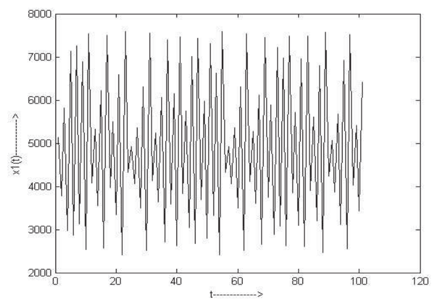

Fig. 5: Chaotic behavior of $X_1(t)$ vs time for β_{ii} =0.05

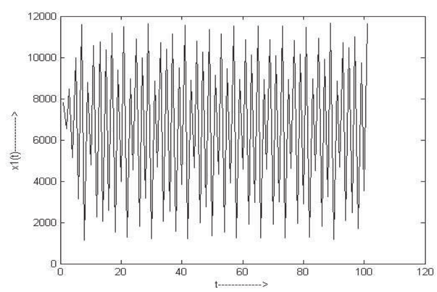

Fig. 6: Chaotic behavior of $X_1(t)$ vs time for λ_{ik} =0.00009

C PHASE PORTRAITS

The chaos and limit cyclic behavior of the proposed antibody–antigen interactive dynamics (6-9) can be best represented by phase portraits. We construct phase portraits

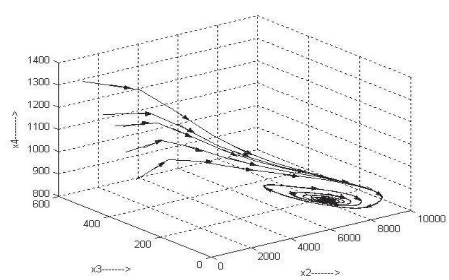

Fig. 7: Phase portraits of X_2, X_3, X_4.with different initial conditions, converging to a stable focus.

of three variables, although there are four antibodies. This is because of our limitations of geometric representation beyond three variables. Fig. 7, 8 and 9 provide phase portraits of the said dynamics for different parameter settings, indicating stable, limit cyclic and chaotic behaviors.

It is clear from Fig. 7 that for different initial values of the antibodies X_1, X_2, X_3, and X_4 the phase portrait converges to a single stable focus [23]. A stable limit cycles in the dark region of the portrait is visible in Fig. 8. The random fluctuations of the antibody concentration in different directions, resulting in a brush-like structure, refer to a chaotic behavior of the dynamics.

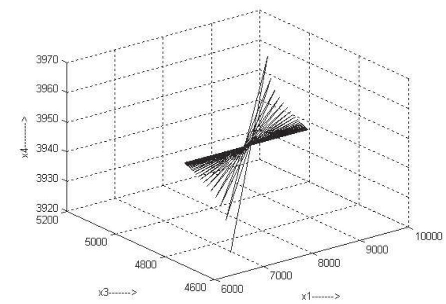

Fig. 8: Phase portrait representing Limit cyclic behavior of the dynamics

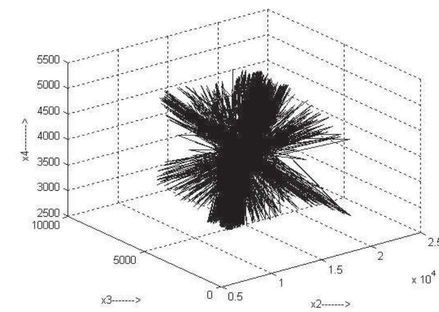

Fig. 9: Phase portrait representing chaotic behavior of the dynamics.

IV LYAPUNOV METHOD FOR STABILITY ANALYSIS

To analyze the condition for stability for the proposed dynamics (1), reproduced below, we intuitively consider a Lyapunov function L (x_i, x_j, x_k, y_m).

$$\frac{dx_i}{dt} = a_{ii} X_i (1 - \frac{X_i}{K}) + \sum_{\exists j} b_{ji} X_i (1 - \exp(-\beta_{ji} X_j))$$
$$- \sum_{\exists k} c_{ki} X_i (1 - \exp(-\lambda_{ik} X_k)) + \sum_{\exists m} z_{im} X_i Y_m$$

Here,

L (x_i, x_j, x_k, y_m)=

$$- \sum_{i=1}^{N} \int_0^{X_i} (a_{ii} (1 - \frac{\xi_i}{K}) + \sum_{\exists j} b_{ji} (1 - \exp(-\beta_{ji} X_j))$$
$$- \sum_{\exists k} c_{ki} (1 - \exp(-\lambda_{ik} X_k)) + \sum_{\exists m} z_{im} Y_m) \xi_i \, d\xi_i$$

We first show that L (x_i, x_j, x_k, y_m) is a Lyapunov energy function, subject to a condition, and then verify that the time derivative of L for the given dynamics is negative.

In order for L (x_i, x_j, x_k, y_m) to be a Lyapunov energy function, we verify that

1. L (0, 0, 0, 0) =0

.2. The partial derivatives: $\frac{\partial L}{\partial X_i}, \frac{\partial L}{\partial X_j}, \frac{\partial L}{\partial X_k}, \frac{\partial L}{\partial Y_m}$ all exist.

3. Further, L (x_i, x_j, x_k, y_m) > 0 will be satisfied if

$$a_{ii} X_i (1 - \frac{X_i}{K}) > [-\sum_{\exists j} b_{ji} X_i (1 - \exp(-\beta_{ji} X_j)) + \sum_{\exists k} c_{ki} X_i (1 - \exp(-\lambda_{ik} X_k)) - \sum_{\exists m} z_{im} X_i Y_m] \quad (10)$$

Now, to test the stability of the dynamics we evaluate

$$\frac{dL}{dt} = \sum_{i=1}^{N} \frac{\partial L}{\partial X_i} \cdot \frac{dX_i}{dt}$$

$$= -\sum_{i=1}^{N} [a_{ii} X_i (1 - \frac{X_i}{K}) + \sum_{\exists j} b_{ji} X_i (1 - \exp(-\beta_{ji} X_j)) - \sum_{\exists k} c_{ki} X_i (1 - \exp(-\lambda_{ik} X_k)) + \sum_{\exists m} z_{im} X_i Y_m] \cdot \frac{dX_i}{dt}$$

$$= -\sum_{i=1}^{n} (\frac{dX_i}{dt})^2 < 0$$

Since dL/dt < 0, the dynamics is asymptotically stable [8]. Since the condition for stability depends on the inequality (10), the stable behavior of the dynamics can be used for applications after ensuring satisfaction of (10).

Example 1: With parameters as listed in Tables I and II, we verify that

$$\frac{dL}{dt} = -[333.8266 - 2.4210 - 89.2414 + 161.4133]^2$$

$$= -[403.5775]^2 < 0.$$

Since dL/dt < 0, we say that the system is conditionally stable.

V STUDY OF CHAOTIC BEHAVIOR WITH LYAPUNOV EXPONENT

TABLE I
INITIAL SETINGS OF VARIABLES

Xi	X1=500	X2=700	X3=500	X4=700
Yi	Y1=300	Y2=400	Y3=500	Y4=300

TABLE II
PARAMETER SETINGS OF THE DYNAMICS

a_{ii}	b_{ji}	c_{ki}	β_{ji}	λ_{ik}	z_{ii}
a_{11}=0.03;	b_{31}=0.9	c_{12}=0.55	β_{31}=0.006	λ_{21}=0.0035	z_{11}=0.001
a_{22}=0.0831	b_{12}=0.2;	c_{23}=0.4	β_{12}=0.001	λ_{32}=0.005	z_{22}=0.001
a_{33}=0.245	b_{32}=0.3	c_{32}=0.5	β_{32}=0.007	λ_{23}=0.005	z_{33}=0.001
a_{44}=0.31;	b_{42}=0.3;	c_{31}=0.45	β_{42}=0.001	λ_{13}=0.005	z_{44}=0.001
	b_{23}=0.4	c_{34}=0.3	β_{23}=0.005	λ_{43}=0.005	
	b_{34}=0.4	c_{42}=0.35	β_{34}=0.001	λ_{24}=0.0035	

In this section, we study chaos with the help of Lyapunov exponent, the definition of which is given below (equation (11)):

$$\lambda = \lim_{N \to \infty} \frac{1}{N} \sum_{n=1}^{N} \ln \left| \frac{d(X_{n+1})}{dX_n} \right|. \quad (11)$$

When λ is greater than 1, the given dynamics is said to be chaotic. Let us now consider the non-linear dynamics given in (5). A discrete approximation of the above dynamics can be obtained by replacing

$$\frac{dXi}{dt} = \frac{Xi(t+1) - Xi(t)}{(t+1) - t}$$

$$= Xi(t+1) - Xi(t) \quad (12)$$

Substitution of (12) in (1) yields the following dynamics:

$$X_1(t+1) = a_{11} X_1 (1 - \frac{X_1}{K}) + b_{31} X_1 (1 - \exp(-\beta_{31} X_3)) - c_{12} X_1 (1 - \exp(-\lambda_{21} X_2)) + z_1 X_1 Y_1 \quad (13)$$

Differentiating $X_1(t+1)$ with respect to $X_1(t)$ we obtain,

$$\frac{dXi(t+1)}{dXi(t)} = a_{11} X_1 (1 - \frac{X_1}{K} + \frac{1}{a_{11}}) + b_{31} (1 - \exp(-\beta_{31} X_3)) - c_{12} (1 - \exp(-\lambda_{21} X_2)) + z_1 Y_1 \quad (14)$$

In order to ensure chaos, we therefore need to satisfy:

$$\frac{dX_1(t+1)}{dX_1(t)} > 1$$

or,

$$a_{11} X_1 (1 - \frac{X_1}{K} + \frac{1}{a_{11}}) + b_{31} (1 - \exp(-\beta_{31} X_3)) - c_{12} (1 - \exp(-\lambda_{21} X_2)) + z_{11} Y_1 > 1 \quad (15)$$

Example 2: In this example we verify that the given dynamics exhibits chaotic behavior for the set of parameters listed in TABLES I and III. The evaluation of dXi (t+1)/dXi (t), for t=0 to 10000, were undertaken and found to be positive throughout. For convenience, we just give a plot of dXi (t+1)/dXi (t), for the first N=10 iterations (Fig 10). The chaotic behavior of the dynamics for the selected range of parameters is apparent.

TABLE III
PARAMETER SETINGS FOR CHAOS

a_{ii}	b_{ji}	c_{ki}	β_{ji}	λ_{ik}	z_{ii}
a_{11}=0.33;	b_{31}=0.9	c_{12}=0.55	β_{31}=0.006	λ_{21}=0.0035	z_{11}=0.0048
a_{22}=0.0831	b_{12}=0.2;	c_{23}=0.4	β_{12}=0.001	λ_{32}=0.005	z_{22}=0.0048
a_{33}=0.245	b_{32}=0.3	c_{32}=0.5	β_{32}=0.007	λ_{23}=0.005	z_{33}=0.0048
a_{44}=0.31;	b_{42}=0.3;	c_{31}=0.45	β_{42}=0.001	λ_{13}=0.005	z_{44}=0.0048
	b_{23}=0.4	c_{34}=0.3	β_{23}=0.005	λ_{43}=0.005	
	b_{34}=0.4	c_{42}=0.35	β_{34}=0.001	λ_{24}=0.0035	

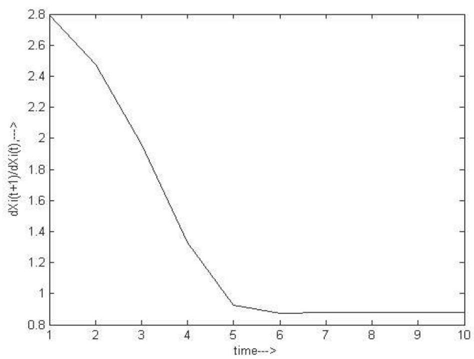

Fig 10: A segment of the graph dXi (t+1)/dXi (t) to demonstrate that the Lyapunov exponent is positive even for very large N (iterations).

VI APPLICATION OF THE STABLE BEHAVIOR OF THE DYNAMICS IN GARBAGE CLEANING BY A MOBILE ROBOT

The stable behavior of the antibody dynamics described in the previous sections has successfully been applied to garbage cleaning by a mobile robot. The garbage-cleaning problem in the present context refers to pick-up of the garbage spread over a given workspace, and their collection and placement in a can located at a specific site of the robot's world map. The robot used for garbage cleaning has to determine obstacle-free trajectories from its current position to the location of the can in the workspace, so that the trajectories pass through a site containing garbage. In the process of locomotion, if the robot loses its battery power it has to recharge its battery from its nearest home base located at a specific site in the robot's world map. So when the battery power level goes below a threshold, the robot attempts to move towards its home base to charge up its battery. In this example, we consider four antigens such as Garbage in front (GF), Garbage in hand (GH), Obstacle is in front (OF), Garbage is in left (GL), and eleven antibodies including Power level high (PLH), Transfer garbage into bin (TGB), Turn right (TR), Turn left (TL), Power down (PD), Wall in left (WL), Obstacle in right (OR), Obstacle in left (OL), Move Forward (MF), Pick up garbage (PUG), Hold the garbage until bin is reached and transfer the garbage into bin (HGB).

A small list of antigen and their corresponding effective antibody and co-operative and competitive counterparts are included in TABLE V. It may added here that on seeing an antigen, the robot fixes the co-efficient a_{ii} , b_{ji}, c_{ki} ,and z_{im} of the dynamics ((6)-(9)), such the stability of the system is ensured. The selections of parameters taken up as an action of an antibody in response to an antigen have been fixed experimentally to avoid possible limit cyclic and chaotic behavior of the dynamics. The strength of antigen has been assumed to be constant. The initial strength of the antibodies is assumed randomly, satisfying the condition for stability (10) and parametric settings as listed in TABLE V. After the dynamics of the antibodies converge, the antibody with the highest strength is considered favorably to execute the necessary task allocated to the given antibody.

Example 3: In the present context, the robot finds garbage in front (Fig. 11); the antibody dynamics of the robot immediately senses the antigen and sets in its necessary parameters in order to attain a stable state. The necessary parameters that ensure stable states are predetermined through experiments. After the dynamics attains a stable or equilibrium state [8], the antibody with highest strength in steady state is determined as the solution to the problem, and the action part implied by the antibody is executed by the robot.

TABLE V
PARAMETRIC CONDITION OF THE PROPOSED ANTIGEN ANTIBODY INTERACTIONS TO ENSURE THE GIVEN RULE OF ACTION

Antigen	Antibody (Rule of action)	Co-operative antibody	Competitive antibody	Parameter conditions
GF	(PUG)	(PLH)	HGB,TL,TR,OR etc	$a_{11}>a_{22},a_{33},a_{44}$
GH	TGB	PLH, MF etc.	TR,TL, OR etc.	$a_{22}>a_{11},a_{33},a_{44}$
OF	TR	PLH,MF	TL,WL	$a_{33}>a_{11},a_{22},a_{44}$
GL	TL	PLH,MF	TR,OL	$a_{44}>a_{11},a_{22},a_{33}$

To illustrate the action of the garbage-cleaning robot, we consider an instance of the robot's world map as indicated in Fig. 11. Here the robot finds garbage in its next state. On sensing the antigen (garbage in front), the robot sets in the parameters of the dynamics autonomously. Then following the first row of TABLE V, the antibody 'Pick up the garbage' and its co-operative and competitive partners, as listed in the first row, become active. The dynamics therefore starts progressing towards a stable point (focus). Once it is attained (Fig. 12(a)), we note that the antibody PUG denoted by X_1 has got the highest strength compared to its competitive antibodies, i.e. Hold the garbage until bin is reached and transfer the garbage into bin (X_2), Obstacle in front (X_4), and co-operative antibody i.e. Power is high (X_3). Therefore the action part of an antibody X_1 (pick up the garbage) is executed. After picking up the garbage, the robot senses another antigen (garbage can is in front). Immediately on sensing this antigen, the robot fixes the parameters of its dynamics as set by the user and all the four antibodies X_1 through X_4 become active following the second row of TABLE V. After the dynamics converges to an equilibrium state, we note that X_2 is higher than X_1, X_3 and X_4 (Fig. 12(b)) following which the robot decides to execute the action part of antibody X_2. Details of the evaluation of the rules of actions of the antibodies, given in TABLE V, can't be presented here for lack of space; we just provide two figures (Fig. 12(c) and (d)) to demonstrate the stable focus of convergence of the dynamics for different initial states of antibodies corresponding to rule of actions listed in the last two rows of TABLE V.

VI. CONCLUSIONS

In this paper, we proposed a new approach to model antigen-antibody interactions, including co-operation and competition of the antibodies. The non-linear dynamics considered for antigen-antibody interaction has been found to demonstrate chaotic, limit cyclic and stable behavior for different parameter settings of the dynamics. The stable behavior of the dynamics has been employed in a garbage cleaning operation by a mobile robot. The parameters of the dynamics that ensure stability are selected through experiments and presented as components of a rule in the presence of specific antigens. The strength of antigens, which in Example 3 has been assumed to be constant, can, in general, have temporal variations. The values of the antibody/antigen concentration, however, have to be determined through measurements for a practical implementation of the system.

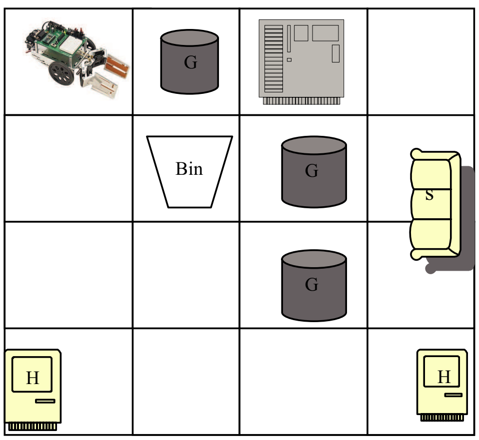

Fig 11: world map of the garbage-collecting robot.

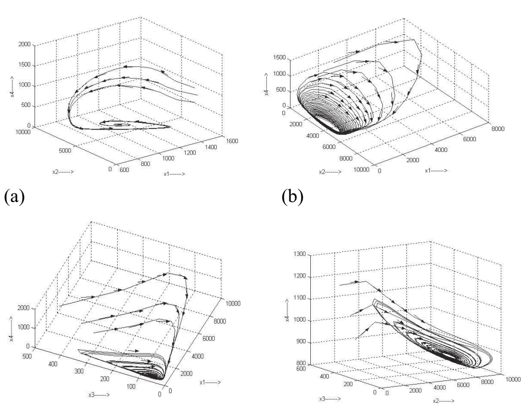

(a) (b) (c) (d)

Fig 12: Convergence of multiple initial points to a fixed stable focus to determine the antibody with the highest strength a_{ij}

REFERENCES

[1] Dasgupta D (ed), Artificial Immune Systems and their applications, 1999, Springer-Verlag

[2] Dasgupta D,Cao Y,Yang C, "An immunogenic approach to spectra recognition," Proc of GECCO 99, pp. –149-155 , 1999

[3] Dasgupta D, "Artificial neural network and artificial immune syllabus: similarities and differences," Proc of the IEEE SMC 1: 873-878, 1997.

[4] Ishida Y, Hariyama H, Fujita H, Ishiguro A, Mori K (eds), Immunity-Based Systems –Intelligent Systems by Artificial Immune Systems, Corona pub., Co. Japan, 1998.

[5] Ishguru A , Watanable Y, Kundo T. and Uchikawa Y, Artificial immunes Network and its Application to Robotics , in soft computing for intelligent Robotics systems , Jain L.C. and Fukuda T, (Eds).

[6] Timmis J, Artificial Immune Systems: A Novel Data Analysis techniques inspired by the immune Network theory. Ph. D. Dissertation, Department of computer Science Univ of Wales, 2000.

[7] de Castro LN, Timmis J, "Artificial immune systems as a novel soft computing paradigm," Springer-Verlag, 2003.

[8] Benjamin C.Kuo, Automatic Control systems, (7th ed), Prentice-Hall of India, 1995.

[9] Langston, CG. (Ed) Artificial life: An overview, MIT press, Cambridge, Massachusetts, 1995.

[10] Taylor. C and Jefferson. D, Artificial life as a tool for biological inquiry, in artificial life: An overview, Langston, C.G (Ed), MIT press, Massachusetts, 1995.

[11] D.Xu and J.C.Principe, "Dynamical analysis of neural oscillators in an olfactory cortex model," Neural Netw, vol.23, pp. 46-55, 2000.

[12] de Castro LN, Timmis J, A novel paradigm for pattern recognition, In: Artificial Neural Networks in pattern recognition, Alonso L, Corchado J, Fyfe C (eds), pp. 67-84, University of Piaseley, 2002.

[13] de Castro LN,Von Zuben FJ, An improving pruning technique with restart for the Kohenen self organizing feature map, 1999.

[14] de Castro LN,Von Zuben FJ, "The Clonal selection algorithm with app.," Proc of GECCO'00, workshop preceding, pp. 36-37, 2000.

[15] de Castro LN,Von Zuben FJ: "An evolutionary immune Network for data clustering," proc. of the ISEE Brazilian Symposium on network, pp. 84-80, 2000.

[16] de Castro LN,Von Zuben FJ, Artificial immune systems : Part – II – A Survey of applications, Technical report – RT DCA 02/00, pp. 65. [On line] www.dca.fee.unicamp.br/~Inunes, 2000.

[17] de Castro LN, Von Zuben FJ, "Immune and neural Network models: theoretical and empirical comparisons," Int at Journal of Computer Intelligence and Applications 1 (3):pp. 239-257, 2001.

[18] de Castro LN, Von Zuben FJ, "An immunological approach to initialize feed forward neural Network weights," 2001.

[19] A.Konar, Computational Intelligence:Principles, Techniques and Applications, Springer, 2005

[20] Clinet: An artificial immune Network for data analysis. in data mining : A Heuristics approach, Abbass HA, Sarkar RA, Network CS(eds), Idea Group publishing, USA, chapter XII. pp.(231-259), 2001.

[21] D. Harter, R. Kozma, "Chaotic Neurodynamics for Autonomous Agents." IEEE Trans. on neural networks, vol.16, no.3, pp. 565-579, May 2005.

[22] Alex A Freitas, J.Timmis, "Revisiting the Foundations of Artificial Immune Systems for data mining." IEEE Trans. On Evolutionary computation, vol. 11, no.4, pp. 521-539 August 2007.

[23] Ogata K, Modern Control Engineering.Englewood Cliffs, NJ: Prentice-Hall, 1987.

[24] Lakhmi C.Jain, Toshio Fukuda, Soft Computing for Intelligent Robotic Systems, Physica-Verlag, pp.-36.